Supporting Information for the Manuscript Entitled

The effect of Vitamin C and iron on dopamine-mediated free radical generation: implications to Parkinson's Disease

Yingying Sun, An Ninh Pham and T. David Waite*

School of Civil and Environmental Engineering, The University of New South Wales, Sydney, NSW 2052, Australia

Keywords: Ascorbate, Iron, Dopamine, Parkinson' disease, Oxidative stress, Quinones

Re-submitted

Dalton Transactions

January, 2018

* Corresponding author. Professor T. David Waite, Tel.: +61 2 9385 5059, Email: d.waite@unsw.edu.au

SI 1 Materials and Methods

All analytical grade chemicals were purchased from Sigma-Aldrich (or as otherwise stated) and were used without further refinement. All solutions were prepared using 18 MΩ.cm ultrapure Milli-Q water (MQ). All glassware was acid washed in 5% (v/v) HCl for at least one week before use. Stock solutions were kept in dark bottles and were refrigerated at 4 ^{o}C when not in use. All experiments were conducted under dark conditions and performed at a controlled room temperature of 22 ± 0.6 ^{o}C.

Solutions were prepared at pH 7.4 by adding an appropriate amount of concentrated NaOH and HCl to buffer solutions containing 0.1 M NaCl, 2 mM $NaHCO_3$ and 10 mM buffer solution. MOPS was used to measure the formation of $Fe^{III}DA_2$ complex and H_2O_2 and decay of ascorbate (Asc) as it does not have spectrum broaden effects. HEPES was used to measure the oxidation of Fe(II) as it does not have significant influence on the measurement in the presence of desferrioxamine B (DFB). All pH measurements were conducted using a Hanna HI9025 pH meter combined with a glass electrode and Ag/AgCl reference. Calibration of the pH electrode was undertaken using NIST buffer solutions (pH 7.01 and 10.01). Experiments were conducted in darkness with the reactor covered in foil for the duration of the reaction.

A concentrated Fe(II) stock solution (5 mM) was prepared by dissolving ferrous ammonium sulfate hexahydrate ($Fe(NH_4SO_4)_2 \cdot 6H_2O$) in 10 mM HCl. Concentrated stock solutions of 10 mM Fe(III) (using ferric chloride hexahydrate ($FeCl_3 \cdot 6H_2O$)) and 10 mM dopamine (DA) were prepared weekly in 10 mM HCl. A concentrated Asc stock solution (200 mM) was prepared daily by dissolving L-ascorbic acid in 50 mM HCl. The working solutions of Fe(II), Fe(III), DA and Asc were diluted from the concentrated stock solutions daily in 10 mM HCl solution. The acidity of both concentrated stock and working solutions was sufficient to avoid significant oxidation of Fe(II), DA and Asc and precipitation of Fe(III) on the time scale of interest and yet low enough to minimize any pH change that might occur on addition of the stock to experimental solutions. A stock solution of 20 mM H_2O_2 prepared by dilution of a nominal 30% w⁄w H_2O_2 solution was used for calibration of the H_2O_2 measurements. The nominal 30% w⁄w solution was standardized by UV spectrophotometry at 240 nm.[1] Concentrated stock solutions of 80 mM ferrozine (FZ) and 20 mM desferrioxamine B (DFB) were prepared in MQ. A daily prepared mixture containing 50 mM FZ and 5 mM DFB was used for Fe(II) determination. Stock solutions of 60 mM N,N-diethyl-*p*-phenylenediamine (DPD) and 500 KU/L horseradish peroxidase (HRP) were prepared in MQ water as described previously.[2] A 100 U/ml ascorbate oxidase (AO) solution was prepared by dissolve AO in MQ water and stored in a -81 ^{o}C freezer when not in use.

Measurement of Fe(II) concentration

The concentration of Fe(II) was quantified spectrophotometrically using the modified FZ method[3] in a 1 cm cuvette by a Cary 60 spectrophotometer at 562 nm and baseline corrected at 690 nm. FZ was chosen because it reacts extremely rapidly with Fe(II) to form a

stable purple complex ($Fe^{II}FZ_3$) with a maximum absorbance at 562 nm and molar absorptivity of $\varepsilon_{562\ nm}$ = 30,000 $M^{-1}cm^{-1}$.[4, 5] However, in the presence of organic complexing reagents, FZ can facilitate reduction of both free and organically complexed Fe(III) resulting in the over prediction of Fe(II) concentration in the samples. Thus, 200 µl DFB containing mixture solution was added to minimize reduction of Fe(III) in the presence of FZ. Since a small amount of Fe(III) was reduced by FZ even in the presence of DFB and contribute to the absorbance at 562 nm, in addition to the calibration of Fe(II), calibration of Fe(III) was also conducted. The concentration of Fe(II) was then calculated using the equation reported previously.[3]

$$[\mathrm{Fe(II)}] = \frac{A_{562} - \varepsilon_{\mathrm{Fe(III)}}[\mathrm{Fe}]_T}{\varepsilon_{\mathrm{Fe(II)}} - \varepsilon_{\mathrm{Fe(III)}}} \qquad \text{(S1)}$$

Where A_{562} represents absorbance at 562 nm, $\varepsilon_{Fe(II)}$ represents molar absorption coefficient of $Fe^{II}FZ_3$ at 562 nm, $\varepsilon_{Fe(III)}$ represents the molar absorption coefficient of the small amount of $Fe^{II}FZ_3$ formed by reduction of Fe(III) in the presence of FZ, and $[Fe]_T$ represents the total Fe concentration.

For the reduction of ferric iron in the presence of Asc in deoxygenated solutions, a special gas mixture of 297 ± 6 ppm CO_2 in argon (BOC) was used to sparge the solution for at least 1 h before the addition of Fe(III) and Asc. Sparging was continued during the course of the experiment in order to maintain deoxygenated conditions.

Measurement of Asc concentration

According to Buettner,[6] the decay of Asc was determined by measuring the decrease in the absorbance at 265 nm with baseline correction at 690nm. The measurement was performed in a 1 cm cuvette by using a Cary 60 spectrophotometer. The molar absorptivity at 265 nm is 14500 $M^{-1}cm^{-1}$ and may vary slightly with pH. The spectrum of Asc as well as the calibration curve is shown in Fig. S1.

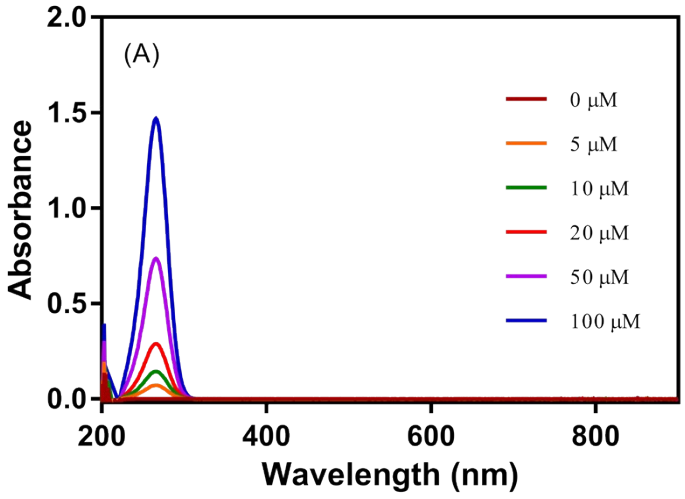

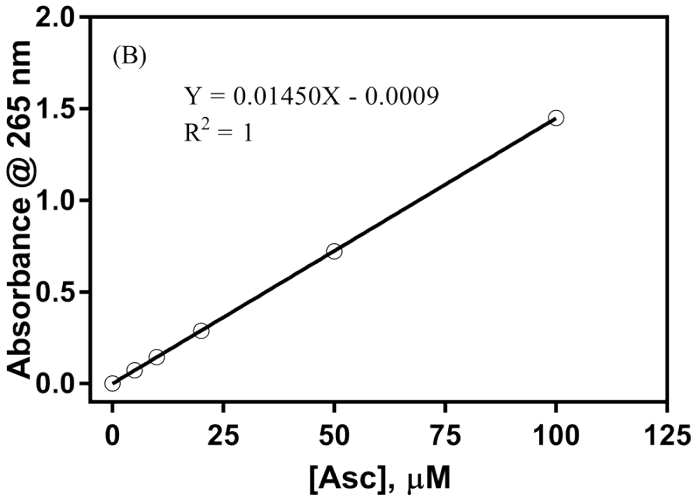

Fig. S1 Measured absorbance of Asc (panel A) and calibration curve for quantification of Asc measured at 265 nm with baseline correction at 690 nm (panel B) in 0.1 M NaCl, 2 mM $NaHCO_3$ and 10 mM MOPS.

Measurement of H_2O_2 concentration

The H_2O_2 formed during the course of Asc oxidation both in the absence and presence of DA was quantified using the modified DPD method.[2] Briefly, in the presence of DPD and HRP, the concentration H_2O_2 was a function of DPD radicals, which has a strong absorbance at 551 nm. However, the presence of Asc can totally scavenge the DPD radicals, resulting in the elimination of H_2O_2 signals as a result of the excellent reducing property. As such, AO was added into the solution before the addition of DPD and HRP to convert all the Asc residuals into DHA and H_2O.[7] The system was calibrated by adding standard H_2O_2 stock into the buffer solutions containing Asc and AO, along with a zero standard containing 60 μM DPD and 500 U/L HRP. Interference arising from the presence of Asc and AO was found to be not significant under the experimental conditions investigated herein (shown in Fig. S2).

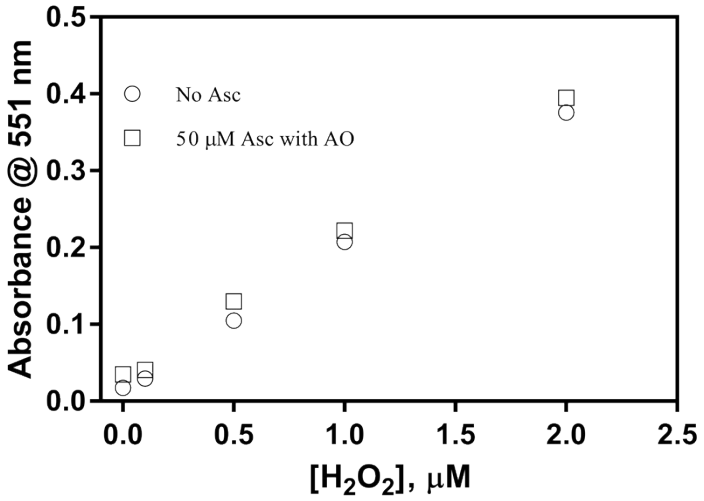

Fig. S2 Measured absorbance of H_2O_2 at 551 nm with baseline correction at 690 nm in 0.1 M NaCl at pH 7.4 in 10 cm cuvette (○) in the absence of Asc and (□) in the presence of 50 μM Asc and sufficient AO.

Fig. S2 indicated that adding sufficient AO before the addition of DPD and HPR can totally convert the Asc into DHA and H_2O, resulting in negligible influence on the H_2O_2 measurement in the presence of Asc.

Measurement of $Fe^{III}DA_2$ complex

The concentration of the *bis*-complex of iron and DA ($Fe^{III}DA_2$) was determined spectrophotometrically in a 10 cm cuvette by measuring the absorbance at 580 nm with baseline correction at 850 nm.[8, 9] The measurements were performed by using a Cary 60 spectrophotometer. Calibration curves for quantification of the concentration of the $Fe^{III}DA_2$ complex were developed under deoxygenated conditions to prevent any oxidation and transformation of the complex.[10] The molar absorptivity of $Fe^{III}DA_2$ was calculated to be 3,121 $M^{-1}cm^{-1}$, which is quite consistent with the previously published value. Given the low concentrations and the small molar absorptivity of the *mono*-complex, the effect of this species on the measurement should be minimal. Considering the pH investigated herein and DA concentration used in this study, the formation of the *tris*-complex should be negligible. Even though the *mono*-complex of Asc and Fe(III) (denoted hereafter as $Fe^{III}Asc$) was considered to be formed, no absorbance was observed at 580 nm (data measured were not shown herein). This observation is consistent with previous studies,[11, 12] in which this complex was assigned with a molar absorptivity from ~11 $M^{-1}cm^{-1}$ at 560 nm to ~325 $M^{-1}cm^{-1}$ at 545 nm. With such a small molar absorptivity, the influence of micromolar concentrations of $Fe^{III}Asc$ on the absorbance at 580 nm should be negligible.

SI 2 Model for the interaction between iron and DA and justification

Modified kinetic model of interaction between iron and DA

Table S1 Modelled reactions and rate constants for the autoxidation of DA at pH 7.4

No.	Reactions	Rate constants ($M^{-1}s^{-1}$ or s^{-1})	Reference
1	$DA + O_2 \xrightarrow{k_1} O_2^{\bullet-} + DA^{\bullet-}$	$k_1 = 8.24 \times 10^{-3}$ [a]	This study
2	$DA^{\bullet-} + O_2 \underset{k_{-2}}{\overset{k_2}{\rightleftharpoons}} DAQ + O_2^{\bullet-}$	$k_2 = 2.95 \times 10^3$	Ref[13]
		$k_{-2} = 1.0 \times 10^9$	Ref[13]
3	$DA^{\bullet-} + DA^{\bullet-} \xrightarrow{k_3} DA + DAQ$	$k_3 = 2.35 \times 10^8$	Ref[14]
4	$DAQ \xrightarrow{k_4} DAL$	$k_4 = 4.45$ [a]	This study
5	$DAL + DAQ \xrightarrow{k_5} DA + DAC$	$k_5 = 5.30 \times 10^6$	Ref[15]
6	$DAL + O_2 \xrightarrow{k_6} DAC + H_2O_2$	$k_6 = 5.12$ [a]	This study
7	$DA^{\bullet-} + O_2^{\bullet-} \xrightarrow{k_7} DAQ + H_2O_2$	$k_7 = 8.27 \times 10^9$ [b]	Ref[10]

Note: a: modified value for the model developed at pH 7.4 in Sun and co-works,[10] b: rate constant taken from Sun and co-works [10] without modification;
DA, dopamine; $DA^{\bullet-}$, dopamine semiquinone radical; DAQ, dopamine-*o*-quinone; DAC, dopaminochrome; DAL, leukoaminochrome and $O_2^{\bullet-}$, superoxide

Table S2 Modelled reactions and rate constants for Fe(III)-catalyzed oxidation of DA at pH 7.4

No.	Reactions	Rate constants ($M^{-1}s^{-1}$ or s^{-1})	Reference
8	$Fe(III) + Fe(III)_I \xrightarrow{k_8} AFO + nH^+$	$k_8 = 5.0 \times 10^6$	Ref[16]
9	$>Fe(III)_n + DA \xrightarrow{k_9} >Fe(III)_{n-1} + Fe^{III}DA$	$k_9 = 2.34$ [b]	Ref[10]
10	$>Fe(III)_n + DA \xrightarrow{k_{10}} >Fe(III)_{n-1} + Fe(II) + DA^{i-}$	$k_{10} = 0.6$ [b]	Ref[10]
11	$Fe(III) + DA \underset{k_{-11}}{\overset{k_{11}}{\rightleftharpoons}} Fe^{III}DA$	$k_{11} = 4.15 \times 10^5$ [a] $k_{-11} = 0.46$	This study This study
12	$Fe^{III}DA + DA \underset{k_{-12}}{\overset{k_{12}}{\rightleftharpoons}} Fe^{III}DA_2$	$k_{12} = 4.5 \times 10^5$ $k_{-12} = 2.59 \times 10^{-4}$	Ref[17] This study
13	$Fe^{III}DA + O_2^{\bullet-} \xrightarrow{k_{13}} Fe^{II}DA + O_2$	$k_{13} = 1.5 \times 10^8$ [b]	Ref[10]
14	$Fe^{III}DA \xrightarrow{k_{14}} Fe(II) + DA^{\bullet-}$	$k_{14} = 0.23$	Ref[18]
15	$Fe^{III}DA_2 \xrightarrow{k_{15}} Fe(II) + DA + DA^{\bullet-}$	$k_{15} = 7.26 \times 10^{-5}$ [b]	Ref[10]
16	$Fe(III) + O_2^{\bullet-} \underset{k_{-16}}{\overset{k_{16}}{\rightleftharpoons}} Fe(II) + O_2$	$k_{16} = 1.5 \times 10^8$ $k_{-16} = 0.77$ [b]	Ref[19] Ref[10]
17	$>Fe(III)_n + O_2^{\bullet-} \xrightarrow{k_{17}} >Fe(III)_{n-1} + Fe(II) + O_2$	$k_{17} = 3.7 \times 10^5$ [b]	Ref[10]

Note: a: modified value for the model developed at pH 7.4 in Sun and co-works,[10] b: rate constant taken from Sun and co-works [10] without modification.

DA, dopamine; $DA^{\bullet-}$, dopamine semiquinone radical; DAQ, dopamine-*o*-quinone; $O_2^{\bullet-}$, superoxide; Fe(III), inorganic ferric ion; $Fe(III)_I$, total inorganic Fe(III); AFO, ferrihydrite and Fe(II), inorganic ferrous ion

Table S3 Modelled reactions and rate constants for Fe(II)-catalyzed oxidation of DA at pH 7.4

No.	Reactions	Rate constants ($M^{-1}s^{-1}$ or s^{-1})	Reference
18	$Fe(II) + O_2^{\bullet-} \xrightarrow{k_{18}} Fe(III) + H_2O_2$	$k_{18} = 1 \times 10^7$	Ref[19]
19	$Fe(II) + H_2O_2 \xrightarrow{k_{19}} Fe(III) + {}^{\bullet}OH + OH^-$	$k_{19} = 1.33 \times 10^4$	Ref[20]
20	$Fe(II) + DA \underset{k_{-20}}{\overset{k_{20}}{\rightleftharpoons}} Fe^{II}DA$	$k_{20} = 7.5 \times 10^{2}$ [b]	Ref[10]
		$k_{-20} = 1.6 \times 10^{-3}$	This study
21	$Fe^{II}DA + O_2 \xrightarrow{k_{21}} Fe^{III}DA + O_2^{\bullet-}$	$k_{21} = 1.45 \times 10^{2}$ [b]	Ref[10]
22	$Fe^{II}DA + H_2O_2 \xrightarrow{k_{22}} Fe^{III}DA + {}^{\bullet}OH + OH^-$	$k_{22} = 1.33 \times 10^4$	Ref[20]
23	$Fe^{II}DA + O_2^{\bullet-} \xrightarrow{k_{23}} Fe^{III}DA + H_2O_2$	$k_{23} = 1 \times 10^{7}$ [b]	Ref[10]
24	$Fe^{II}DA + DA^{\bullet-} \xrightarrow{k_{24}} Fe^{III}DA + DA$	$k_{24} = 1.92 \times 10^{5}$ [b]	Ref[10]

Note: a: modified value for the model developed at pH 7.4 in Sun and co-works,[10] b: rate constant taken from Sun and co-works [10] without modification.

DA, dopamine; $DA^{\bullet-}$, dopamine semiquinone radical; $O_2^{\bullet-}$, superoxide; Fe(III), inorganic ferric ion; Fe(II), inorganic ferrous ion; H_2O_2, peroxide and ${}^{\bullet}OH$, hydroxyl radicals

Model justification

Given the relatively complicated model developed in this study, several intermediates were measured in order to have a better constraint for the rate constants used and proposed herein. Briefly, the decay of Asc and the generation of H_2O_2 (shown in Fig. 1) are used for the constraint of the autoxidation of Asc and the interaction between $DA^{\bullet-}$ and Asc. The decay of Asc in the presence of iron coupled with the oxidation of Fe(II) and the formation of Fe(II) from Fe(III) both in the absence and presence of O_2 (shown in Figs. 2 and 3) are used for the constraint of the interaction between iron and Asc with emphasis on the formation of iron-Asc complexes and the surface interactions. Finally, the ligand competition as well as the ligand exchange between Asc and DA for both Fe(II) and Fe(III) is constrained by the results shown Figs. 4 and 5. Discussion of factors underpinning the selection of each rate constant is provided below. Sensitivity analysis is used to determine the importance of the reactions proposed in this study.

As shown in Fig. S3A, in view of the scavenging of ROS, the oxidation of Asc by O_2 and $O_2^{\bullet-}$ are much more important processes than that of $^{\bullet}OH$ as the relative residuals *r* are considerable sensitive to the change in the orders of magnitude of rate constants. The apparent shift point as a suggestion of the sensitivity analysis coupled with the theoretical calculation using the intrinsic oxidation rate constants proposed by Marcus theory (main text) indicate that the proposed rate constant for the oxidation of Asc by O_2 should be reasonable. Accordingly, the convergence of the adopted rate constant of the oxidation of Asc by $O_2^{\bullet-}$ with the sensitive point suggested by the sensitivity analysis confirms that the value used herein should be reasonable. In comparison, a relatively insensitive relative residual *r* is observed for the interaction between Asc and $^{\bullet}OH$, which may mainly attribute to the experimental conditions used in this study. Theoretically, the high concentrations of organic buffer used here should efficiently quench the $^{\bullet}OH$ generated during the course of the experiment. As such, given the common sense, while insensitive, the interaction between Asc and $^{\bullet}OH$ is kept in the model in this work.

As shown in Fig. S3B, compared with the interaction between $AA^{\bullet-}$ and $O_2^{\bullet-}$, the disproportionation of $AA^{\bullet-}$ and the reduction of DHA by $O_2^{\bullet-}$ are much more important processes as a result of the sensitive relative residual *r* to the change in the rate constants over several orders of magnitude. The convergence of the shift points with the values used here indicates that the adopted and proposed rate constants for these two processes should be reasonable. The insensitivity of the scavenging of $O_2^{\bullet-}$ by $AA^{\bullet-}$ to the change in the rate constant suggests that the value adopted from previous study can only be treated as an upper limit for this process.

As shown in Fig. S3C, in general, the formation of iron-Asc complexes, including AFO, Fe(III) and Fe(II), is critical process for the considerable sensitivity of relative residuals *r* to the change in the rate constants over several orders of magnitude. The agreement of the sensitive points with the proposed rate constants indicates that the values used here should be reasonable. In comparison, the relative insensitivity of the formation of the surface

complex between AFO and Asc below the proposed value suggests that the rate constant proposed herein can only be treated as an upper limit for this process.

As shown in Fig. S3D, as a result of the internal electron transfer, both surface bound Fe(II) and aqueous Fe(II) can be generated from the surface bound and aqueous $Fe^{III}Asc$ complexes with these processes accompanying the concomitant release of $AA^{\bullet-}$. The considerable sensitivity of the relative residuals *r* to the change in the orders of magnitude of rate constants indicates that these two processes should be important. Compared with internal electron transfer within the aqueous $Fe^{III}Asc$ complex, the proposed value for the surface bound complex should only be treated as the lower limit as a result of the general insensitivity of the relative residual *r* to the change in the rate constant greater than the proposed value.

Theoretically, the transformation of ferric iron could be mediated by the active radicals. As shown in Fig. S3E, compared with the reduction of ferric iron by $AA^{\bullet-}$, the reduction of $Fe^{III}Asc$ by $O_2^{\bullet-}$ is generally not important for the insensitivity of the relative residual *r* to the change in the rate constant over several orders of magnitude. As such, to simplify the complicated model, while considerably thermodynamic favourable, the reduction of $Fe^{III}Asc$ by $O_2^{\bullet-}$ is not included in the model developed in this study. Despite converged at the same point, the reduction of $Fe^{III}Asc$ by $AA^{\bullet-}$ is much more sensitive to the change in the rate constant than that of Fe(III). This phenomenon may be attributed to the ready precipitation of aqueous Fe(III), which renders a considerably lowered availability of Fe(III).

In view of the fate of the surface bound Fe(II), there are three main pathways, which are the re-oxygenation and the diffusion both in the absence and presence of Asc. As shown in Fig. S3F, the considerable insensitivity of the relative residual *r* to the change in the rate constant below the proposed values suggests that the values describing the diffusion processes can only be treated as the upper limits for these two processes. As a common sense, the oxidation of surface bound Fe(II) should be remarkably faster than that in the aqueous compartment. As such, even though the proposed value for the oxidation of surface bound Fe(II) can only be treated as the lower limit, the value proposed herein should be reasonable in view of the surface catalyzed oxidation.

In a manner similar to the inorganically bound ferrous iron, theoretically, the Asc bound Fe(II) can be oxidized by O_2, $O_2^{\bullet-}$ and H_2O_2. As shown in Fig. S3G, compared with the oxidation by $O_2^{\bullet-}$, the oxidation of $Fe^{II}Asc$ by O_2 and H_2O_2 are much more important processes for the considerable sensitivity of relative residuals *r* to the change in the rate constants over several orders of magnitude. The convergence of the proposed rate constant for the oxidation of $Fe^{II}Asc$ by O_2 as well as the adopted rate constant for the oxidation of $Fe^{II}Asc$ by H_2O_2 with the sensitive point suggested by the sensitivity analysis indicate that the values used herein should be reasonable. According to the rate law:

$$-\frac{d[Fe^{II}Asc]}{dt} = k_{Fe^{II}Asc+O_2^{\bullet-}}[Fe^{II}Asc][O_2^{\bullet-}] \quad \text{(S2)}$$

the considerable insensitivity of the relative residual *r* to the change in rate constant may be mainly attributed to the trace concentrations of $O_2^{\bullet-}$, which renders the $O_2^{\bullet-}$ mediated pathway being less important. To simplify the complicated model developed in this study, the oxidation of Asc bound Fe(II) by $O_2^{\bullet-}$ is not included in the model reactions.

As discussed in the main text, the presence of Asc plays an important role in view of the alleviation in the progression of PD via the mediation in the transformation of DA related toxicants. As shown in Fig. S3H, the $AA^{\bullet-}$ induced scavenging of $DA^{\bullet-}$ as well as the Asc related reduction of DAQ are important processes as a result of the sensitivity of the relative residuals *r* to the change in the orders of magnitude of the rate constants. The convergence of the adopted rate constant for the reduction of DAQ by Asc with the shift point obtained by the sensitivity analysis indicates that the values used herein should be reasonable. In contrast, the general insensitivity of the relative residual *r* below the proposed value suggests that the value of $AA^{\bullet-}$ induced reduction of $DA^{\bullet-}$ should only be treated as the upper limit.

As shown in Fig. S3I, compared with the surface Asc bound Fe(III), the ligand exchange process between aqueous Fe^{III}Asc and DA is much more important for the considerable variation of the relative residual *r* to the change in the rate constant over several orders of magnitude. The generally insensitivity of the relative residual *r* below the proposed value for the surface ligand exchange process indicates that the value should only be treated as the upper limit.

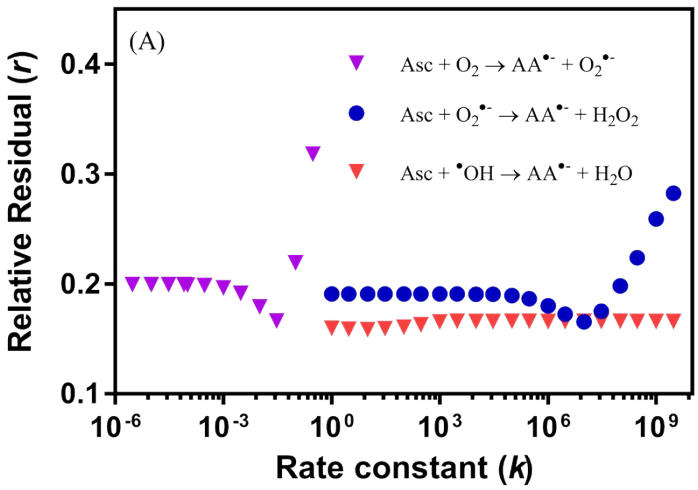

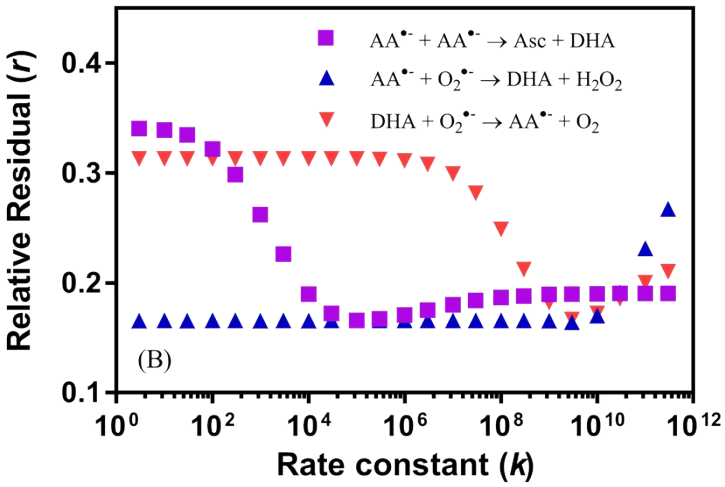
Relative Residual (r)
0.4
0.3
0.2
0.1
AA•- + AA•- → Asc + DHA
AA•- + O2•- → DHA + H2O2
DHA + O2•- → AA•- + O2
(B)
10^0 10^2 10^4 10^6 10^8 10^10 10^12
Rate constant (k)

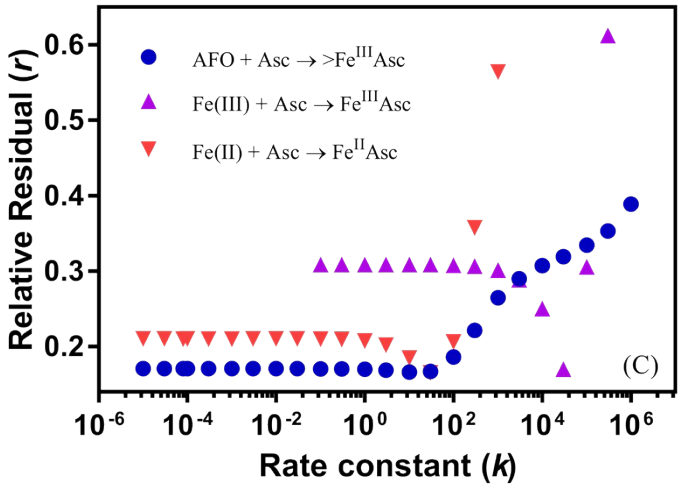
Relative Residual (r)
0.6
0.5
0.4
0.3
0.2
AFO + Asc → >Fe^III Asc
Fe(III) + Asc → Fe^III Asc
Fe(II) + Asc → Fe^II Asc
(C)
10^-6 10^-4 10^-2 10^0 10^2 10^4 10^6
Rate constant (k)

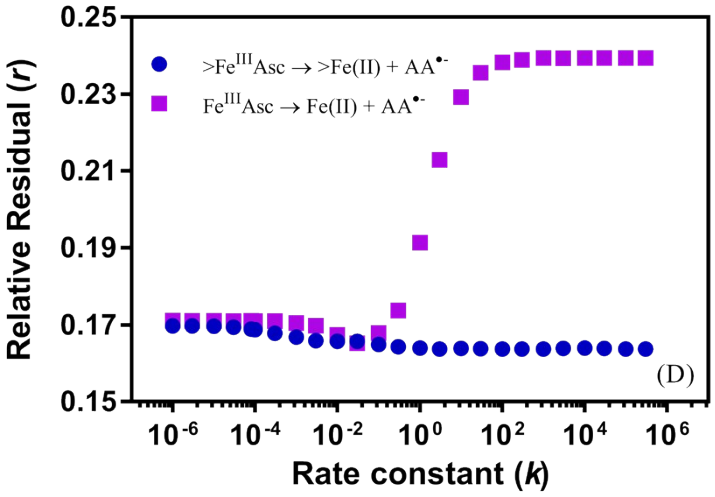
Relative Residual (r)
0.25
0.23
0.21
0.19
0.17
0.15
>Fe^III Asc → >Fe(II) + AA•-
Fe^III Asc → Fe(II) + AA•-
(D)
10^-6 10^-4 10^-2 10^0 10^2 10^4 10^6
Rate constant (k)

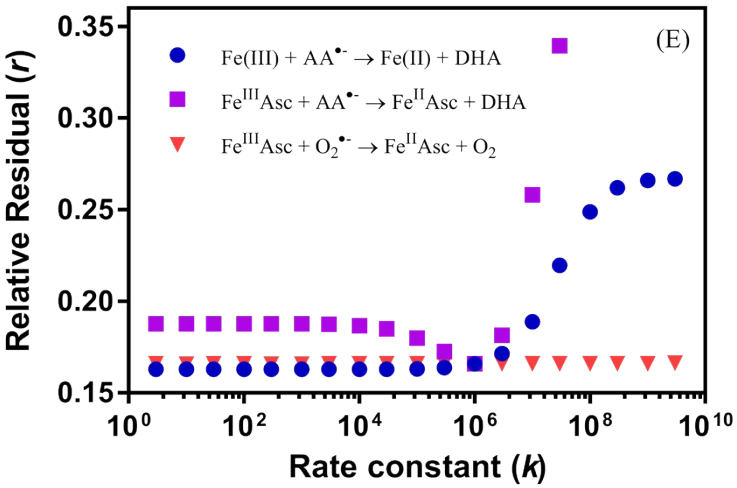
(E)
Fe(III) + AA•- → Fe(II) + DHA
FeIIIAsc + AA•- → FeIIAsc + DHA
FeIIIAsc + O2•- → FeIIAsc + O2
Relative Residual (r)
Rate constant (k)

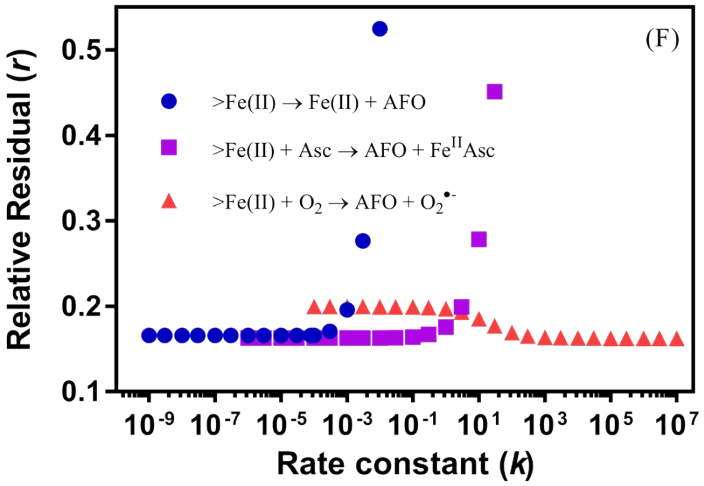
(F)
>Fe(II) → Fe(II) + AFO
>Fe(II) + Asc → AFO + FeIIAsc
>Fe(II) + O2 → AFO + O2•-
Relative Residual (r)
Rate constant (k)

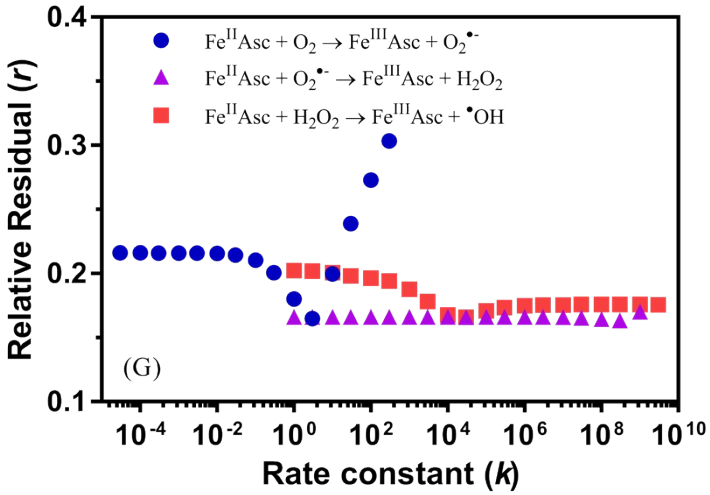
FeIIAsc + O2 → FeIIIAsc + O2•-
FeIIAsc + O2•- → FeIIIAsc + H2O2
FeIIAsc + H2O2 → FeIIIAsc + •OH
(G)
Relative Residual (r)
Rate constant (k)

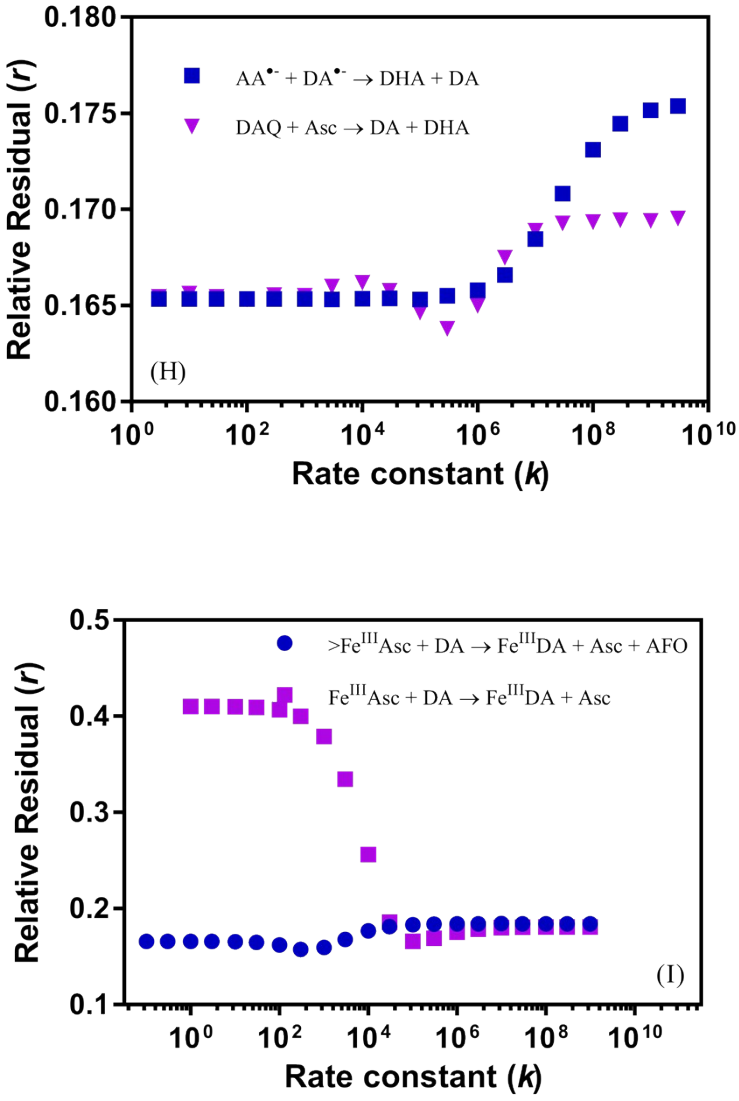

Figure S3. Sensitivity analysis for the rate constants used for the reactions shown in Tables 1 – 4 in the main text.

SI 3 Oxidation pathway of ascorbate in the absence of added metals

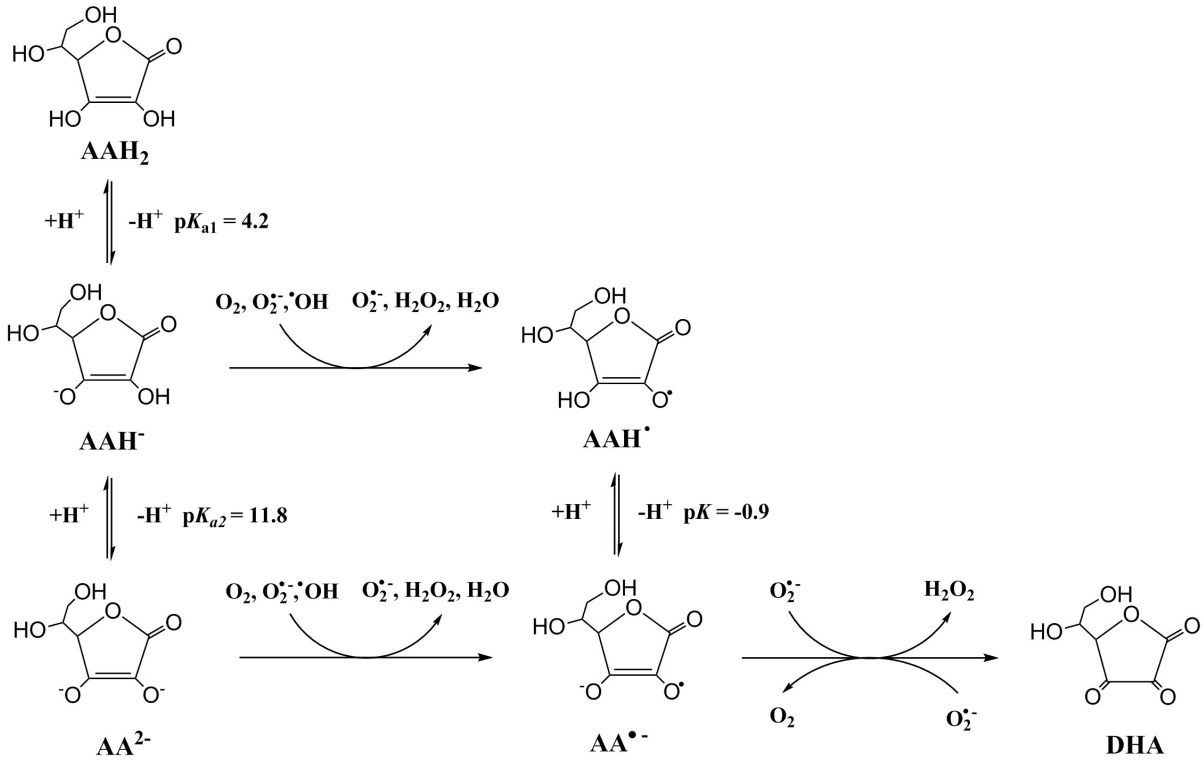

Figure S4 Oxidation pathway of Asc in the absence of added metals.

Under physiological condition pH 7.4, given the two pK_a values (pK_{a1} = 4.2 and pK_{a2} = 11.8),[21] the ready deprotonation of one hydrogen of Asc renders AAH^- being the dominant species. Possessing the extremely low pK_a value, once being oxidized, the ascorbate semiquinone would be deprotonated with resultant all the ascorbate semiquinone present as $AA^{\bullet-}$.

SI 4 Supplementary data

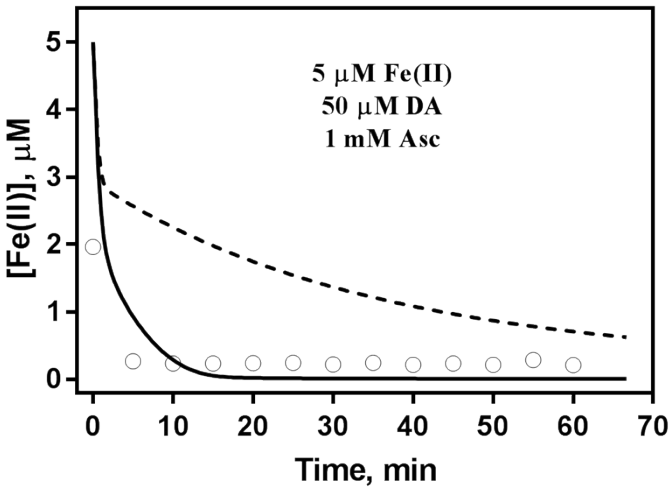

Figure S5 Oxidation of 5 μM Fe(II) in the presence of 50 μM DA and 1 mM Asc at pH 7.4 in 0.1 M NaCl. The solid line represents the model fitting including the peroxidation of $Fe^{II}Asc$ and the dashed line represents the model fitting without the peroxidation of $Fe^{II}Asc$.

Reference

1. M. S. Morgan, P. F. Van Trieste, S. M. Garlick, M. J. Mahon and A. L. Smith, *Anal Chim Acta*, 1988, **215**, 325-329.
2. H. Bader, V. Sturzenegger and J. Hoigne, *Water Res*, 1988, **22**, 1109-1115.
3. S. Garg, H. Ito, A. L. Rose and T. D. Waite, *Environ Sci Technol*, 2013, **47**, 1861-1869.
4. L. L. Stookey, *Anal Chem*, 1970, **42**, 779-781.
5. E. Viollier, P. Inglett, K. Hunter, A. Roychoudhury and P. Van Cappellen, *Appl Geochem*, 2000, **15**, 785-790.
6. G. R. Buettner, *J Biochem Bioph Meth*, 1988, **16**, 27-40.
7. G. M. Greenway and P. Ongomo, *Analyst*, 1990, **115**, 1297-1299.
8. A. Avdeef, S. R. Sofen, T. L. Bregante and K. N. Raymond, *J Am Chem Soc*, 1978, **100**, 5362-5370.
9. M. J. Sever and J. J. Wilker, *J Chem Soc, Dalton Trans*, 2004, 1061-1072.
10. Y. Sun, A. N. Pham and T. D. Waite, *J Neurochem*, 2016, **137**, 955-968.
11. G. Laurence and K. Ellis, *J Chem Soc, Dalton Trans*, 1972, 1667-1670.
12. P. Martinez, J. Zuluaga, D. Uribe and R. Van Eldik, *Inorg Chim Acta*, 1987, **136**, 11-16.
13. A. N. Pham and T. D. Waite, *J Inorg Biochem*, 2014, **137**, 74-84.
14. J. Borovansky, R. Edge, E. J. Land, S. Navaratnam, S. Pavel, C. A. Ramsden, P. A. Riley and N. P. Smit, *Pigm Cell Res*, 2006, **19**, 170-178.
15. E. Land, S. Ito, K. Wakamatsu and P. Riley, *Pigm Cell Res*, 2003, **16**, 487-493.
16. A. N. Pham, A. L. Rose, A. J. Feitz and T. D. Waite, *Geochim Cosmochim Acta*, 2006, **70**, 640-650.
17. M. A. Blesa and E. Matijević, *Adv Colloid Interfac*, 1989, **29**, 173-221.
18. U. El-Avaan, E. Herlinger, R. Jameson and W. Linert, *J Chem Soc, Dalton Trans*, 1997, **16**, 2813-2818.
19. J. D. Rush and B. Bielski, *J Phys Chem*, 1985, **89**, 5062-5066.
20. M. González-Davila, J. M. Santana-Casiano and F. J. Millero, *Geochim Cosmochim Acta*, 2005, **69**, 83-93.
21. J. Du, J. J. Cullen and G. R. Buettner, *Biochimica et Biophysica Acta (BBA)-Reviews on Cancer*, 2012, **1826**, 443-457.